Iranian Journal of Pharmaceutical Sciences
2026: 22 (1): 192-207
https://journals.sbmu.ac.ir/IJPS

Research Article

# Fabrication and Characterization of Soframycin-Loaded Carboxymethyl Tamarind Gum-Guar Gum Hydrogel Films

Vishwajeet Sampatrao Ghorpade[a], Kailas Krishnat Mali[b] *, Vijay Daulatrao Havaldar[c], Afroj Usman Shikalkar[b], Om Santosh Varude[b], Remeth Jacky Dias[d]

[a] *Krishna Institute of Pharmacy, Krishna Vishwa Vidyapeeth (Deemed to be University), Karad-415539, Maharashtra, India.*
[b] *Department of Pharmacy, Adarsh Institute of Pharmacy, Bhavaninagar, Vita-Kundal Road, Vita, Tal- Khanapur 415311 Dist- Sangli, Maharashtra, India.*
[c] *Department of Pharmaceutics, Adarsh College of Pharmacy, Vita, Near MIDC, Khambale (Bha.), Tal- Khanapur 415311 Dist- Sangli, Maharashtra, India.*
[d] *Department of Pharmacy, Government College of Pharmacy, Karad 415124 Dist- Satara, Maharashtra, India.*

**Received:** July 13, 2025 **Last Revision:** October 14, 2025 **Accepted:** January 26, 2026 **Available online:** June 15, 2026.

**Abstract**

Hydrogel films fabricated solely from citric acid (CA)-crosslinked carboxymethyl tamarind gum (CMTG) often suffer from poor matrix integrity and limited swelling capacity, hindering their practical utility in drug delivery and other biomedical applications. To address these challenges, this study developed hydrogel films by blending CMTG with guar gum (GG) and crosslinking with citric acid, aiming to enhance the films' matrix integrity and swelling behavior substantially. The hydrogel films were loaded with soframycin via diffusion. The fabricated films were evaluated for various parameters, including weight loss, thickness, total carboxyl content, wettability, permeability, protein adsorption, and hemocompatibility. The swellability of the films was studied in Tris-HCl buffer (pH 7.4) and 0.1 N HCl. In addition, drug release studies were conducted in Tris-HCl buffer (pH 7.4). The films were characterized using ATR-FTIR spectroscopy and thermal analysis. The findings revealed that the concentrations of GG and CA affected the weight loss, thickness, total carboxyl content, and contact angle. The swelling of CMTG-GG hydrogel films was found to be greater than that of previously reported CMTG-PVA films. The fabricated films exhibited optimum water vapor transmission and microbial impermeability. Protein adsorption on the hydrogel films remained minimal.

Additionally, the hemolysis percentage remained below the accepted limit of 5 %, confirming that the hydrogel films were compatible with blood. The ATR-FTIR analysis confirmed the crosslinking. The drug release from the soframycin-loaded hydrogel films was found to be 39.1 % to 79.69 % at the end of 6 h. The drug release from these hydrogel films followed a non-Fickian diffusion mechanism. These findings suggest that hydrogel films composed of CMTG and GG have promising potential for drug delivery.

*Keywords*: Carboxymethyl tamarind gum; Citric acid; Crosslinking; Guar gum; Soframycin.

*** Corresponding Author**:
**Kailas Krishnat Mali**, Department of Pharmaceutics, Adarsh College of Pharmacy, Near MIDC, Khambale (Bha.), Vita Tal- Khanapur 415311 Dist- Sangli, Maharashtra, India. E-mail: malikailas@gmail.com.

**Cite this article as**: Ghorpade V.S., Mali K.K., Havaldar V.D., Shikalkar A.U., Varude O.S., Dias R.J. Fabrication and Characterization of Soframycin-Loaded Carboxymethyl Tamarind Gum-Guar Gum Hydrogel Films. Iran. J. Pharm. Sci., 2026, 22 (1): 192- 207.

DOI: https://doi.org/10.22037/ijps.v22i1.48978

## 1. Introduction

Topical drug delivery is often the method of choice for localized treatment because it is simple to use and cost-effective compared to other methods. This approach involves applying medication directly to the surface areas of the body, such as the skin, eyes, nasal passages, or vaginal region, and targeting the site of action more directly. Topical delivery bypasses the liver's first-pass metabolism and helps reduce variability in drug levels in the bloodstream [1]. Over the past few decades, scientists worldwide have been developing novel drug delivery systems to improve the efficiency of traditional medications. The goal is to make treatments safer, more effective, and easier for patients [2]. Oral medications have various problems, such as repeated dosing, difficulty in maintaining therapeutic levels, and systemic toxicity. To overcome these challenges, researchers have explored novel drug delivery systems, such as hydrogels [3].

Lee, Kwon, and Park coined the word "hydrogel" in 1849 [4]. Hydrogels are biocompatible, crosslinked, three-dimensional (3D) polymeric networks defined by their height, breadth, and length. They are composed of hydrophilic polymers that contain up to 90% water [5]. The water-holding capacity of hydrogels is due to the presence of functional groups on polymer structures, such as sulfonic (-$SO_3H$), hydroxyl (-OH), carboxylic (-COOH), amino (-$NH_2$), amide (-CONH), and primary amide (-$CONH_2$) groups [4]. Owing to their distinctive properties, such as biocompatibility, biodegradability, superabsorbency, hydrophilicity, softness, viscoelasticity, and fluffiness, hydrogels play an important role in biomedicine. Hydrogels have been explored in areas such as tissue engineering, drug delivery, personal hygiene products, wound dressing, and wound healing because they can mimic the natural properties of biological tissues [6].

Topical products contain a variety of therapeutic agents to treat skin conditions, such as anesthetics, anti-inflammatory agents, corticosteroids, antibiotics, and antifungals [7]. Soframycin is a broad-spectrum antibiotic effective against gram-positive and gram-negative organisms [8]. It is also known as framycetin sulfate and belongs to the aminoglycoside family [9]. Its molecular formula is $C_{23}H_{48}N_6O_{17}S$, and its molecular weight is 614.64 g $mol^{-1}$ [10]. It appears as a white to off-white, amorphous, hygroscopic, and odorless powder and is freely soluble in water. It inhibits bacterial protein synthesis by irreversibly binding to ribosomal subunits. It is used to treat different skin conditions, including skin infections, minor wounds, burns, and cuts, thereby promoting faster healing and reducing the risk of complications [9].

Hydrogels can be fabricated using natural, synthetic, and semisynthetic polymers [11]. Hydrogels synthesized from natural polymers offer various advantages, including low cost, accessibility, and transparency; however, they have low strength, which may compromise their stability [12]. The performance of hydrogels in drug delivery applications can be improved by combining natural polymers with synthetic or semi-synthetic polymers [13].

Guar gum (GG) is a naturally occurring polymer derived from plants. GG is a non-ionic, inexpensive, linear polysaccharide that appears as a white to yellowish, smooth powder. It is extracted from the endosperm of the seeds of *Cyamopsis tetragonoloba*, a drought-tolerant legume species belonging to the family *Leguminosae*. It is a water-soluble polymer with a large number of hydroxyl groups in its structure and good film-forming ability [14]. GG-derived films have notable limitations, including pronounced brittleness, suboptimal mechanical integrity, elevated hydrophilicity, and insufficient moisture permeability resistance [15].

Carboxymethyl tamarind gum (CMTG) is prepared by modifying tamarind gum (TG) with carboxymethyl groups (–$CH_2$ –COOH), which helps improve its physical and chemical performance. It is a semi-synthetic anionic polysaccharide available at a reasonable price compared to other semi-synthetic derivatives of natural polymers [12]. It consists of D-xylose, D-galactose, and D-glucose in molar proportions of 1:2:3 [16]. CMTG is a biopolymer of choice due to its strong resistance to microbial breakdown and excellent film-forming properties. It also helps reduce the extracellular matrix and shows potential for use in skin tissue-related applications [17]. Researchers have

explored the use of CMTG in various controlled drug delivery systems [18]. Films made from CMTG, gelatin, and TG have been reported in the literature for wound-healing applications [19]. Over the years, CMTG has been used to produce hydrogels, composites, films, and pellets that have been tested in various applications, including agriculture, drug delivery, wastewater treatment, and tissue engineering [16].

Crosslinking is a structural modification technique that connects polymer chains through chemical bonding, thereby improving the strength, stability, and overall functional performance of polymer-based films [15]. A crosslinker forms covalent or ionic linkages between polymer chains, enhancing the stability and matrix integrity of the resulting film [20]. Citric acid (CA) is widely recognized as a nontoxic and cost-effective crosslinking agent for hydrogel development [21]. Upon heating to an appropriate temperature, CA forms covalent intermolecular di-ester bonds with the hydroxyl (-OH) groups of the polymers, resulting in a stable crosslinked network [15].

CMTG hydrogel films crosslinked solely with citric acid (CA) often suffer from poor matrix integrity and limited swelling capacity [12]. Although blending CMTG with synthetic polymers like polyvinyl alcohol (PVA) has shown some improvement, there is a scarcity of studies investigating the combination of CMTG with natural polymers using CA as a crosslinker. Natural polymers hold the potential to enhance both the swelling properties and matrix integrity of CMTG-based hydrogels [11,22]. GG is renowned for its biocompatibility, biodegradability, and excellent film-forming properties [23–25]. Its hydrophilic nature contributes to a high swelling capacity and invasive swelling characteristics, which are advantageous for water retention [26]. By combining CMTG with GG, the strong hydrophilic nature of GG can be leveraged to enhance overall swelling performance [27]. Additionally, guar gum is known to interact with other polymers, resulting in hydrogels with improved mechanical and rheological properties [23–25, 28]. Therefore, it is hypothesized that CA crosslinked CMTG-GG hydrogel films may exhibit superior matrix integrity and swelling performance compared to CMTG hydrogel films.

Soframycin-loaded hydrogel films based on CMTG and GG were prepared using CA as a crosslinker. They were characterized for swelling behavior, water vapor permeability, total carboxyl content, microbial barrier properties, and hemocompatibility. Additionally, the films were evaluated for their drug loading capacity and release kinetics.

## 2. Materials and methods

Research Lab Fine Chem, Mumbai, supplied guar gum. Soframycin (Framycetin Sulphate) was received from Encube Ethical Pvt. Ltd., Goa (India). Citric acid and isopropyl alcohol (IPA) were obtained from Loba Chemie, Mumbai. Chhaya Industries, Barshi, Maharashtra, India, generously supplied the CMTG. All other chemicals utilized in this investigation were of analytical grade and were used as supplied.

### *2.1 Fabrication of CMTG-GG hydrogel films*

Hydrogel films were prepared using a previously reported process with minor modifications. In brief, an aqueous solution of CMTG-GG (2 % w/v) was prepared with constant stirring at 1000–1500 rpm using a magnetic stirrer (Remi, India) at room temperature for 2h. The previously prepared homogeneous solution was mixed with 0.6% w/v citric acid. The solution was then poured into a Petri plate and kept overnight to remove the entrapped air bubbles. The Petri plate was then dried in a hot air oven (Ecogen, Equitron, India) at 50ºC for 24 h. Dried films were cured at 140°C for 10 min to achieve the desired crosslinking between CMTG and GG. The cured films were rinsed with distilled water and IPA. The films were then dried and stored in a desiccator until further use [12]. The composition of the hydrogel matrix is presented in **Table 1**. The effect of CMTG:GG ratio (HG1-HG4), CA concentration (HG3 and HG7), curing temperature (HG3 and HG5), and curing time (HG3 and HG6) on properties of CMTG-GG hydrogel films was studied.

**Table 1.** Composition of CMTG – GG hydrogel films

| Batch | Ratio of CMTG -GG* | CA (% w/v) | Curing temperature (ºC) | Curing time (min) |
|---|---|---|---|---|
| **HG1** | 10:0 | 0.6 | 140º | 10 |
| **HG2** | 9:1 | 0.6 | 140º | 10 |
| **HG3** | 8:2 | 0.6 | 140º | 10 |
| **HG4** | 7:3 | 0.6 | 140º | 10 |
| **HG5** | 8:2 | 0.6 | 145º | 10 |
| **HG6** | 8:2 | 0.6 | 140º | 15 |
| **HG7** | 8:2 | 0.7 | 140º | 10 |

*Concentration of polymer is 2% w/v

*2.2 Percent weight loss and thickness measurement*

The percent weight loss of the crosslinked hydrogel films was determined from the films' practical yield. The practical yield of the hydrogel film was determined by comparing the final weight of the dried film to the initial total weight of the polymers and CA. The thickness of the hydrogel films was measured using a micrometer screw gauge. The average thickness was calculated by measuring the thickness at six different locations of the hydrogel film [11].

*2.3 Wettability study*

The wetting behavior of the hydrogel films was determined using a laboratory-based water contact angle setup. A 10 µL volume of distilled water was placed on the surface of the hydrogel film using a microliter (µL) pipette. A digital camera was used to capture the image of the drop within a few seconds. The captured images were analyzed using ImageJ software [29].

*2.4 Total carboxyl content*

A previously published approach was used to determine the total carboxyl content of the hydrogel films. The total carboxyl content was measured using acid-base titration. A solution of 0.1 N HCl (titrant) and 0.1 N NaOH (titrate) was prepared. Dry hydrogel films (100 mg) were immersed in 20 mL of 0.1 N NaOH and stirred at 200-300 rpm on a magnetic stirrer for 2 h. NaOH helps break down the ester linkages to form a dispersion and reacts with the free carboxyl group to form citrate (sodium carboxylate). Titration was performed by gradually adding 0.1 N HCl to 0.1 N NaOH, with phenolphthalein as the indicator. The total carboxyl content of the hydrogel films was calculated using the following formula:

$$\text{Total carboxyl content (mEq/100g)} = \frac{(V_b\text{-}V_a) \times N \times 100}{W} \quad (01)$$

where N is the normality of HCl, $V_b$ is the volume of HCl in the absence of the sample, $V_a$ is the volume of HCl in the presence of the sample, and W is the weight of the sample in grams [12].

*2.5 Swelling study*

A sA swelling study was performed using a previously reported method with slight modifications. Initially, the weight of a dry hydrogel film (1×1 cm) was recorded. The films were then immersed in Tris-HCl buffer (pH 7.4) and 0.1 N HCl at room temperature. The weights of the swollen hydrogel films were recorded at specific time intervals of up to 1440 min. The excess medium present on the film was blotted with tissue paper, and the swollen hydrogel films were weighed using a moisture balance (Shimadzu, Japan). The swelling ratio was calculated using the following formula:

$$\text{Swelling ratio} = \frac{(W_t - W_0)}{W_0} \quad (02)$$

where $W_t$ is the weight of swollen hydrogel at time T, and $W_o$ is the initial weight of the dry hydrogel films [30].

*2.6 Permeability study of hydrogel film*

*2.6.1 Water vapour permeability study*

The WVTR of the fabricated hydrogel matrix was determined using the desiccation method. For this study, circular sections of the hydrogel film with a 1 cm

diameter were cut. 10 mL glass vials were filled with anhydrous calcium chloride ($CaCl_2$ ), and the hydrogel film pieces were placed over the vial openings using Teflon tape to prevent air from entering. The vials were prepared such that the distance between the surface of the $CaCl_2$ and the inner side of the film was approximately 10 mm. Control vials (reference) were prepared without the hydrogel films. Each vial was weighed and stored in a desiccator containing saturated sodium chloride (NaCl) solution to maintain a constant humidity. The weight of each vial was recorded at specific time intervals up to 72 h using an analytical balance to monitor the water vapor transmission. The water vapor transmission rate was determined using the following formula:

$$\text{WVTR} = \frac{[(\Delta W/\Delta t)\times 24]}{A} \qquad (03)$$

Where, $(\Delta W/\Delta t)$ is the slope obtained from the plot of 'w' vs 't', W is the weight gain (g) along the specific time period, 't'(h), and 'A' is the effective transfer area ($m^2$) [11].

### *2.6.2 Microbial permeation study*

The microbial permeability of the crosslinked hydrogel matrix was also evaluated. The film was secured over the opening of 10 mL vials containing 5 mL of nutrient broth. Films were cut into circular shapes (diameter: 1 cm) and sterilized using an autoclave (Portable pad, Equitron, India). To provide a basis for comparison, both negative (-) and positive (+) controls were prepared. For the positive control, a vial containing 5 mL of nutrient broth was opened to the environment; for the negative control, a vial containing 5 mL of nutrient broth was sealed with a sterile cotton ball. All vials, including positive and negative controls, were placed in an incubator (Ecogen, Equitron, India) for one week under controlled conditions. The vials were checked daily for turbidity or cloudiness, which was identified as microbial contamination [13].

### *2.7 Protein adsorption properties of hydrogel films*

A modified version of the previously reported Lowry method was employed to study the protein adsorption on hydrogel films. Briefly, a 1×1 cm hydrogel film was immersed in Tris-HCl buffer (pH 7.4) containing 200 µg/mL bovine serum albumin (BSA) and incubated at 37°C for 24 h with constant stirring. After incubation, the film was removed and rinsed five times with phosphate buffer. To extract the adsorbed protein, the film was placed in 5 mL of 1% (w/v) sodium dodecyl sulfate (SDS) solution and shaken at 100 rpm on an orbital shaker (Remi, India) for 1 h at 37°C. The resulting solution was appropriately diluted and analyzed using a UV-Vis spectrophotometer (UV-1800, Shimadzu, Japan). For calibration, a BSA stock solution (1 mg/mL) was prepared (Stock I). Serial dilutions ranging from 0.05 to 1 mg/mL were prepared using Tris-HCl buffer (pH 7.4). From each dilution, 0.2 mL was transferred to test tubes containing 2 mL of alkaline copper sulphate reagent, and the mixture was mixed thoroughly. Following a 10-minute incubation period at room temperature, 0.2 mL of Folin-Ciocalteu reagent was added to the solutions. The solutions were then incubated for 30 min. Absorbance was measured at 660 nm using a spectrophotometer, and a calibration curve was constructed by plotting the absorbance against the protein concentration. The protein content in the unknown samples was determined using this calibration curve [30].

### *2.8 Hemolysis assay*

Hydrogel film samples, each with a surface area of 2 $cm^2$, were first allowed to swell in Tris-HCl buffer at 37°C for 1 hour. After removing the Tris-HCl, 0.5 mL of goat blood was added to each sample. After a 20 min incubation period, 4.0 mL of 0.9 % sodium chloride (NaCl) solution was added. The samples were then incubated at 37°C for an additional hour. The mixtures were then centrifuged at 4000 rpm for 10 min. The supernatant was analyzed spectrophotometrically at 545 nm. The following formula was used to determine the percentage of haemolysis:

$$\text{Haemolysis (\%)} = \frac{(A_{test\ sample} - A_{-ve\ control})}{(A_{+ve\ control} - A_{-ve\ control})} \qquad (04)$$

Positive control: 0.5 mL goat CPD blood and 4mL distilled water.

Negative control: 0.5 mL goat CPD blood, 0.9% NaCl saline, and 4mL distilled water.

where A is the absorbance [30].

*2.9 Drug loading and content of hydrogel film*

The hydrogel film (500 mg) was immersed in 50 mL Tris-HCl buffer solution (pH 7.4). For up to twelve hours, the films were left to swell and absorb the medication. After the loading phase, the swollen hydrogel films were removed and dried in a hot-air oven at 40°C for 24 h. Because soframycin has very little UV absorbance, the amount released in Tris-HCl solution was determined by colorimetric analysis. Each dried film (approximately 100 mg) was cut into small pieces and immersed in 50 mL of Tris-HCl buffer (pH 7.4). The solution was stirred continuously at 100 rpm using a magnetic stirrer. The drug solution was filtered, and 5mL was transferred from the filtrate into a 10 mL volumetric flask. Subsequently, soframycin was derivatized to form a colored complex. To a volumetric flask, 0.1 mL of pyridine and 2 mL of ninhydrin reagent were added, and the volume was adjusted to 10 mL with distilled water. The resulting solution was transferred to a separate test tube and heated in a water bath at 65-70 ℃ for 10 min. The test solution was then cooled, and the absorbance of the complex was quantified using a UV–visible spectrophotometer at 400 nm (Shimadzu 1800, Japan) [11, 30].

*2.10 In vitro drug release of hydrogel film*

The drug release study was conducted by placing a soframycin-loaded hydrogel film (1×1 cm, approximately 100 mg) into 20 mL of Tris-HCl buffer solution (pH 7.4) maintained at room temperature. Aliquots were collected at predetermined time intervals and replenished with fresh dissolution medium to ensure sink conditions. Then, 5mL of the sample was pipetted out and transferred to a 10 mL volumetric flask. Pyridine (0.1 mL pyridine and 2mL of ninhydrin reagent were added to each flask, and the remaining volume was adjusted with distilled water. The solution was transferred to a test tube and heated to 65-70 ℃ for 10 min. The cooled solution was then analyzed to determine the amount of soframycin released using a UV spectrophotometer (Shimadzu, Japan).

Release data were fitted to Zero-order, First-order, Higuchi, and Korsmeyer-Peppas models, and the best-fit model was determined from $R^2$ values [31]. The Korsmeyer-Peppas equation was fitted to release data up to 60% of the total drug released to analyze drug release kinetics.

$$kt^n = \frac{M_t}{M_\infty} \quad (05)$$

where $M_t/M_\infty$ represents the fraction of the drug released at a given time t (min), $k$ is the kinetic constant, and $n$ is the diffusion exponent, which reflects the nature of the interaction between the drug and the hydrogel matrix components [30].

*2.11 Characterization of Hydrogel films*

*2.11.1 ATR-FTIR*

The infrared (IR) spectra of soframycin, CMTG, GG, HG1, unloaded HG3, and loaded HG3 hydrogel films were obtained using an ATR-FTIR spectrophotometer (Alpha II, Bruker). The samples were analyzed using ATR-FTIR, with spectra collected over the range of 600 to 4000 $cm^{-1}$ at an average of 25 scans and resolution of 4 $cm^{-1}$ [15].

*2.11.2 Thermal analysis*

A Mettler-Toledo TGA/DSC thermogravimetric analyzer (Mettler-Toledo, Switzerland) was used to perform thermogravimetric analysis (TGA) on CMTG, GG, and CA-crosslinked hydrogel films. The samples were heated from 30ºC to 600ºC at 10ºC/min under a nitrogen atmosphere with a flow rate of 10 mL/min [15].

## 3. Results and discussion

*3.1 Fabrication of hydrogel films*

A CMTG + GG solution containing 2% w/v polymer was prepared. A preliminary study was conducted to determine the optimal concentrations of CMTG, GG, and CA for preparing crosslinked hydrogel films. Using less than 2% w/v CMTG + GG resulted in insufficient crosslinking within the hydrogel film. However, increasing the concentration beyond 2% w/v led to a loss of film integrity, likely due to reduced interpolymer crosslinking between CMTG and GG and increased intrapolymer crosslinking within GG chains. For citric acid (CA), a minimum concentration of 0.6% w/v was required to produce hydrogel films with good integrity

and stability. However, increasing the CA concentration above 0.6 % w/v resulted in hard and brittle films. The films were cured at 140°C for 10 min to form a stable, well-formed hydrogel matrix. This curing step is essential because, at elevated temperatures, CA promotes crosslinking by forming intermolecular diester bonds with the hydroxyl groups present in the polysaccharide structure. The esterification reaction occurs between the cyclic anhydride and the OH group of the CMTG and GG chains.

### *3.2 Mechanism of crosslinked hydrogel films*

In this study, an esterification reaction was used to fabricate a CMTG-GG crosslinked hydrogel film using CA as a crosslinker. Initially, CA was heated with CMTG-GG at 140℃ for 10 min. CA creates covalent intermolecular (between molecules) di-ester linkages with the OH group present in the CMTG-GG structure, forming a crosslinked network. When heat is provided to CA, it is converted into a cyclic anhydride intermediate that allows crosslinking with the polymer chain by esterifying hydroxyl (-OH) groups [12].

### *3.3 Percent weight loss and thickness of the hydrogel films.*

**Table 2** presents the % weight loss of the hydrogel films after washing with water and isopropyl alcohol, along with the thickness measurements of the dried films. The percent weight loss of the hydrogel films ranged from 29.33% to 34.87%. An increase in the concentration of GG (HG2–HG4) caused an increase in the weight loss of the hydrogel films. This weight loss may be due to the large number of free (-OH) groups in GG, which may interact with water and dissolve during the washing stage. When the crosslinking density was increased in batches HG5, HG6, and HG7, the weight loss decreased. This might be due to the strong crosslinking between CMTG, GG, and CA. The thickness was found to be dependent on the weight loss. The film thickness decreased with increasing weight loss. This suggests that the film thickness was influenced by the crosslinking density within the hydrogel structure [11].

### *3.4 Wettability study of film*

The wettability of the prepared hydrogel film was evaluated using ImageJ, and the results are presented in **Table 2** [11]. The contact angle is inversely related to hydrophilicity. A high contact angle (> 90°) indicates the hydrophobic nature of the film, whereas a low contact angle (<90°) indicates the hydrophilic nature [32]. The contact angle was found to be 46.78°–60.94°. **Figure 1** shows the contact angles of all the batches. Batch HG1 of the CMTG hydrogel demonstrated a high contact angle. Adding GG to CMTG decreased the contact angle. As the GG concentration increased (HG2 to HG4), the contact angle decreased. This might be due to the high hydroxyl group content in GG. Increasing the curing temperature in HG5 increased the contact angle. Similarly, when the curing time was increased in HG6, the contact angle increased. Furthermore, the contact angle increased with increasing CA concentration in batch HG7. This might be due to the high crosslinking density, which converts the hydrophilic film into a hydrophobic form [32]. The crosslinked films exhibited hydrophilic behavior, which may be attributed to the large number of hydroxyl groups (-OH) present in CMTG and GG.

**Table 2.** Evaluation of hydrogel films

| Batches | Percent weight loss (%) | Thickness (µm) | Contact angle (°) | TCC (mEq/100g) | WVTR (g/m$^2$) | Microbial Permeability (Day 7$^{th}$) | Protein Adsorption (mg/cm$^2$) | Hemolysis (%) |
|---|---|---|---|---|---|---|---|---|
| HG1 | 29.33±4.78 | 560.33±5.87 | 56.45±1.79 | 290±9.42 | 1017.15 | -ve | 0.048 | 2.771 |
| HG2 | 31.44±5.79 | 553.88±5.66 | 53.75±3.51 | 300±4.71 | 1176.69 | -ve | 0.040 | 2.013 |
| HG3 | 32.64±5.43 | 554.99±3.59 | 48.89±0.63 | 320±4.24 | 1303.58 | -ve | 0.024 | 2.334 |
| HG4 | 34.87±1.24 | 553.89±4.37 | 46.78±0.88 | 340±9.42 | 1335.20 | -ve | 0.008 | 2.480 |
| HG5 | 31.60±4.18 | 556.66±4.78 | 57.72±0.66 | 370±4.71 | 1101.97 | -ve | 0.048 | 3.034 |
| HG6 | 29.51±7.40 | 556.89±3.60 | 60.94±0.27 | 350±9.42 | 938.77 | -ve | 0.056 | 3.938 |
| HG7 | 32.54±3.74 | 554.44±2.07 | 55.24±1.59 | 410±9.35 | 1077.48 | -ve | 0.01 | 4.026 |
| Control | - | - | - | - | 2211.70 | +ve | - | - |

TCC: total carboxyl content; WVTR: water vapour transmission rate. Reading expressed as average ± SD, (n=3)

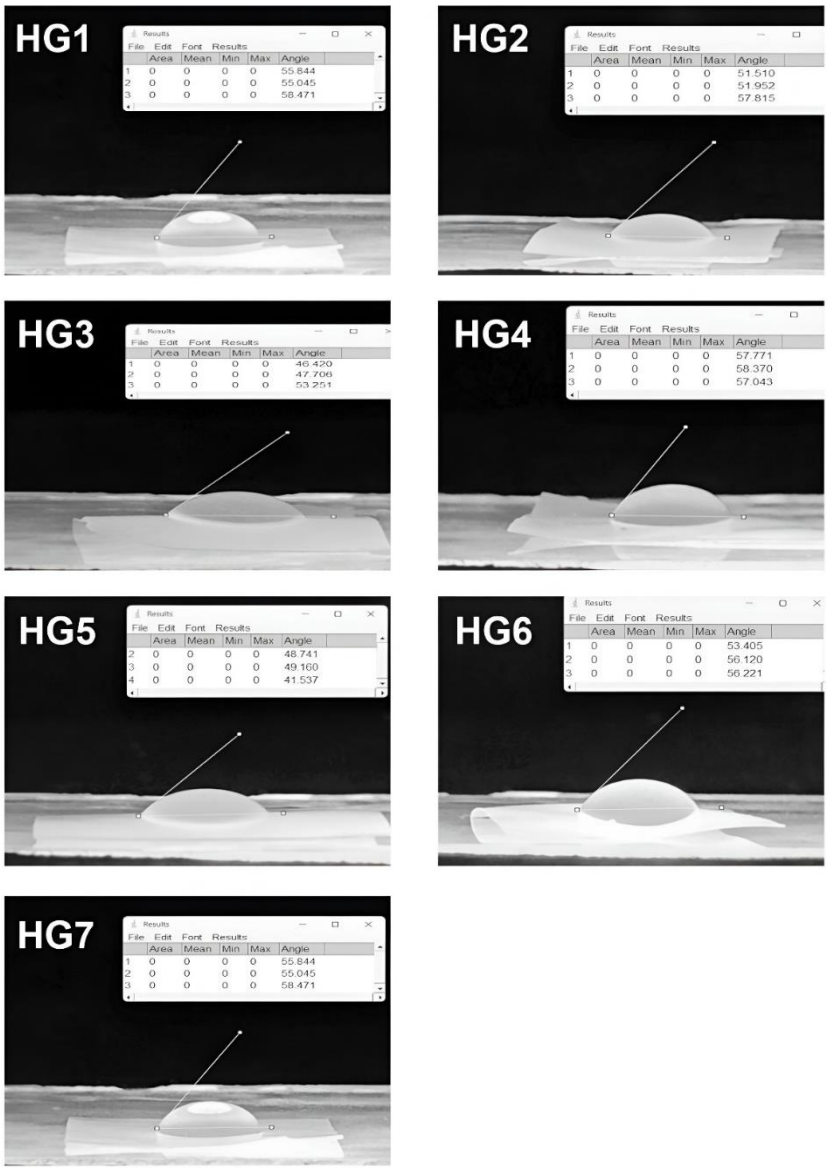


**Figure 1.** Contact angle of all batches (HG1-HG7)

*3.5 Total carboxyl content*

The CA crosslinked CMTG-GG hydrogel films consist of ester carboxylate and free carboxylic groups. When the films were immersed in a sodium hydroxide (0.1N) solution, the sodium hydroxide cleaved the ester crosslink and reacted with the carboxylate to form sodium carboxylate [11]. The polymer concentration, citric acid concentration, curing temperature, and curing time affected the TCC of the hydrogel films.

**Table 2** lists the TCC values for all the hydrogel films. In hydrogel films (HG2-HG4), when guar gum concentration was increased, TCC increased. This could be due to the presence of GG in the esterification reaction with citric acid [25]. The TCC of hydrogel films HG5 and HG6 increased with increasing curing time and temperature. This may be due to the formation of dense crosslinking between the polymer chains [21]. Increasing the CA concentration in batch HG7 also resulted in a higher carboxyl content in the hydrogel films. This may be attributed to increased CA participation, which ultimately increases the polymers' crosslinking density [11].

### 3.6 Permeability study

#### 3.6.1 Water vapour permeability test

The water vapor permeability of the fabricated film is essential for providing a moist environment for wound healing, as it prevents tissue drying [11]. The results of the permeability test for the crosslinked CMTG-GG films are listed in **Table 2**. The water vapor permeability of the crosslinked films was considerably lower than that of an open vial(control). The CA-crosslinked CMTG hydrogel films exhibited a water vapor transmission rate of 1017.15 g/cm², whereas the control exhibited a WVTR of 2211.70 g/cm². The results indicated that as the GG concentration increased from batch HG2 to HG4, the rate of water vapor transmission through the films increased. This behavior can be attributed to the hydrophilic characteristics of GG and CMTG.

Compared to batch HG3, raising the curing temperature in HG5 reduced the WVTR. Similarly, increasing the curing time in batch HG6 further reduced the water vapor transmission rate. Additionally, increasing the CA content in batch HG7 decreased WVTR. This reduction is attributed to greater crosslinking, which reduces the films' porosity and forms a denser network [33].

#### 3.6.2 Microbial permeability study

The results of the microbial permeability test are presented in **Table 2**. The crosslinked hydrogel films were evaluated for microbial permeability by placing them over vials containing nutrient broth and monitoring microbial growth over 1 week. Day 0: No microbial growth was observed in any of the vials, including the positive and negative controls and those sealed with hydrogel films. Day 4: The positive control vials showed turbidity, indicating microbial growth. The negative control remained clear, and all vials sealed with the hydrogel films showed no signs of microbial contamination. Day 7: Both the positive and negative control vials showed microbial growth, whereas the vials covered with hydrogel films remained clear, with no visible signs of microbial growth [11]. The results of microbial permeability testing revealed that the crosslinked hydrogel films effectively prevented microbial permeation, serving as a barrier against contamination from the external environment.

### 3.7 Protein adsorption study

The results of the protein adsorption test for CA-crosslinked CMTG-GG films are presented in **Table 2**. The cell adhesion response is closely linked to the study of protein adsorption on hydrogel films. Albumin, a major protein component of blood, was used in this analysis. In this study, Bovine Serum Albumin (BSA) was used as a model protein to assess the hydrogel films' protein adsorption capacity. The results of the protein adsorption test for the crosslinked CMTG-GG hydrogel films ranged from 0.008 to 0.056 mg/cm². The films exhibited low protein adsorption, attributed to their hydrophilic nature. This hydrophilicity facilitates interactions with water molecules and leads to the repulsion of protein molecules [11]. Overall, the findings indicate that the crosslinked hydrogel films exhibit reduced protein adsorption capacity due to their hydrophilic nature.

### 3.8 Hemocompatibility study

The crosslinked hydrogel films were tested for hemocompatibility using a hemolysis assay. The results of the hemolysis study are presented in **Table 2**. The results showed that the hemolytic activity of all batches of the crosslinked hydrogel films remained within the acceptable limit of 5 %, indicating good hemocompatibility of the hydrogels. In CA-crosslinked CMTG-GG hydrogel films, a slight increase in hemolysis was observed with higher concentrations of guar gum CA and with increased curing temperature and time [11]. Overall, the findings confirmed that all crosslinked batches of CMTG-GG hydrogel films exhibited long-lasting hemostatic potential, making them suitable for hemostatic applications.

### 3.9 Swelling study

Swelling is an essential parameter that influences the drug loading and release behavior of hydrogel films. The effects of GG, CA, curing temperature, and time on the swellability of the hydrogel film were studied in Tris-HCl buffer (pH 7.4). The swelling was measured for up to 24 h after immersion in Tris-HCl buffer (pH 7.4). The results of the swelling study of the hydrogel films are illustrated in **Figure 2A**.

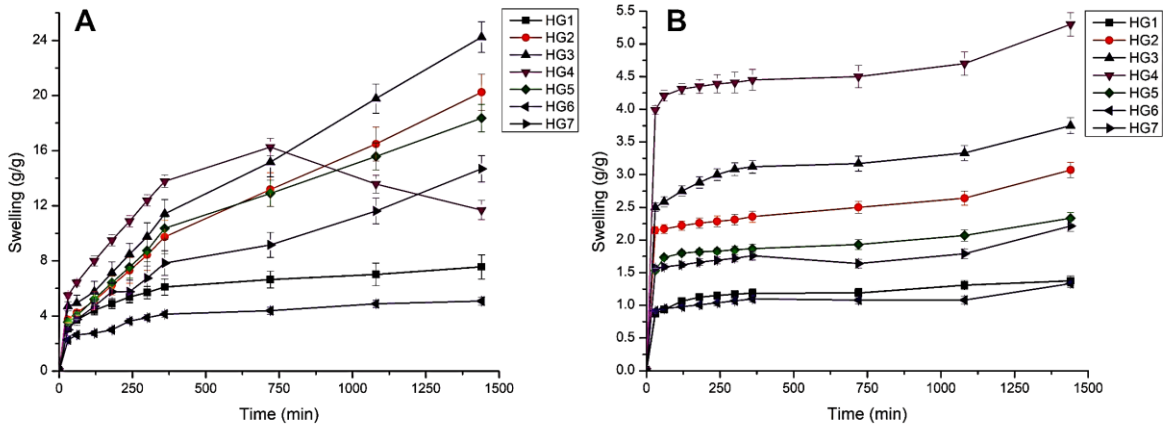


**Figure 2**. Swelling of CMTG-GG hydrogel films in Tris-HCl buffer pH 7.4 (A) and 0.1 N HCl (B)

The results indicated that increasing the guar gum concentration from HG2 to HG4 increased film swelling. Batch HG4 showed good swelling behavior, reaching 16.32 g/g at 12 h. However, after 15 h, the swelling in HG4 decreased. This reduction may be attributed to the higher GG content, which leads to erosion. Exposure of CMTG-GG films to Tris-HCl buffer disrupts their intermolecular hydrogen bonds, thereby reducing their swelling capacity [34].

Batch HG6 showed low swelling due to its high crosslinking density, resulting in a smaller network space and less mobile polymer chains. This resulted in a more rigid polymer structure, reducing the diffusion medium's penetration into the densely crosslinked network [12]. In batch HG3, the highest swelling was observed at the optimum CMTG-GG concentration. The enhanced swelling in batch HG3 may be due to the deprotonation of the carboxyl groups in CA at pH 7.4, leading to the formation of carboxylate ions. These ions generate repulsive forces that increase the distance between interpolymeric chains, thereby improving the film's swelling capacity [11].

When comparing batch HG3 with batch HG5 (higher curing temperature), HG6 (longer curing time), and HG7 (higher CA content), a decrease in the swelling ability of hydrogel films is observed. This was attributed to the formation of a denser crosslinked polymeric network. This suggests that an increase in crosslinking density reduces the swelling of the hydrogel films [35].

To evaluate the effect of pH on the swelling of crosslinked films, a swelling study was conducted in 0.1 N HCl, as shown in **Figure 2B**. The concentrations of GG and CA, as well as the curing temperature and time, significantly influenced the swelling behavior in the acidic medium. All hydrogel batches remained intact and did not erode in 0.1 N HCl solution. Among them, batch HG4 exhibited the highest swelling (5.30 g/g), whereas batch HG6 showed the lowest swelling (1.33 g/g). This may be attributed to the protonation of carboxylate ions in CMTG, which reduces electrostatic repulsion between polymer chains and decreases swelling capacity. The crosslinked films exhibited less swelling in 0.1 N HCl than in Tris-HCl buffer at pH 7.4 [11, 12].

### *3.10 Drug loading and content*

Drug loading in the crosslinked hydrogel films was carried out by diffusion in Tris-HCl buffer (pH 7.4)[30], in which soframycin was diffused into the swollen hydrogel network. The drug loading data are provided in **Table 3**. The swelling behavior of the films directly influences drug loading in crosslinked hydrogel films [11]. The drug-loading capacity of the fabricated crosslinked films ranged from 125.52 to 194.48 mg/g. Among them, film HG4 showed the highest drug loading, whereas batch HG6 exhibited lower drug loading. Increasing the amount of guar gum from HG2 to HG4 improved the drug-loading ability of the crosslinked films. The swelling study results support this trend. The enhanced swelling likely facilitated faster

drug diffusion into the hydrogel network and retention within the matrix [11]. In batches HG5, HG6, and HG7, the enhancement of crosslinking density within the hydrogel matrix resulted in reduced film swelling. Consequently, the limited swelling restricted the diffusion of the drug from the bulk solution into the hydrogel matrix, leading to lower drug loading [12, 13]. The results indicated that the films made with CMTG alone showed low drug loading. However, when CMTG was partially replaced with guar gum (GG), an improvement in drug loading capacity was observed, suggesting that the addition of GG enhanced the ability of the fabricated hydrogel film to absorb and retain the drug in the hydrogel matrix [11, 21].

### *3.11 In vitro drug release study of the fabricated hydrogel films.*

In the present study, crosslinked hydrogel films were developed for drug delivery applications. Therefore, an *in vitro* drug release study of soframycin was conducted using Tris-HCl buffer (pH 7.4) [30]. The results indicated that drug release from the hydrogel films was attributed to their swellability. **Figure 3** shows the release pattern of soframycin from the CMTG-GG crosslinked films.

**Table 3.** Drug loading and release profile of soframycin

| Batch | Drug loading (mg/g) | Drug release $Q_{6h}$ (%)* | Zero order $R^2$ | First order $R^2$ | Higuchi $R^2$ | Korsmeyer-Peppas | | Release mechanism |
|---|---|---|---|---|---|---|---|---|
| | | | | | | $R^2$ | n | |
| HG1 | 152.29±5.48 | 39.21 | 0.656 | 0.447 | 0.851 | 0.997 | 0.63 | Non-Fickian |
| HG2 | 161.35±5.51 | 61.51 | 0.723 | 0.478 | 0.899 | 0.999 | 0.67 | Non-Fickian |
| HG3 | 189.69±6.93 | 77.73 | 0.605 | 0.402 | 0.812 | 0.995 | 0.69 | Non-Fickian |
| HG4 | 194.48±7.24 | 79.69 | 0.586 | 0.392 | 0.796 | 0.996 | 0.71 | Non-Fickian |
| HG5 | 162.92±5.95 | 53.59 | 0.627 | 0.406 | 0.827 | 0.979 | 0.64 | Non-Fickian |
| HG6 | 125.52±4.22 | 55.41 | 0.491 | 0.337 | 0.713 | 0.972 | 0.60 | Non-Fickian |
| HG7 | 163.44±6.01 | 40.57 | 0.668 | 0.442 | 0.860 | 0.982 | 0.59 | Non-Fickian |

*Percent soframycin release at the end of 6 h

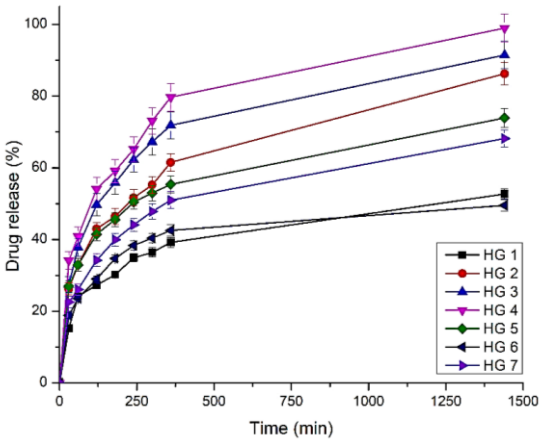


**Figure 3.** In vitro drug release of soframycin from CMTG-GG hydrogel films.

When hydrogel films were placed in the dissolution medium, they exhibited an initial burst release from all drug-loaded hydrogel batches (HG1-HG7). The initial burst release was observed for up to 1h and ranged from 23.58% to 40.86%. This burst release is attributed to the immediate release of the free drug present on the surface of the crosslinked hydrogel film [11, 12]. As the drug-loaded hydrogel films dried, the solvent gradually moved towards the surface and evaporated. It carries drug molecules within the hydrogel matrix to the surface, a phenomenon known as back diffusion. When the dried film is later exposed to the dissolution medium, these surface-accumulated drug molecules are released quickly, leading to an initial burst release effect [21]. As the concentration of GG increased in the CMTG hydrogel films, the drug release from hydrogel batches HG2–HG4 gradually increased. This might be due to an increase in the swelling phenomenon [36]. Hydrogel batches HG5, HG6, and HG7 exhibited greater crosslinking density, which limited their swelling capacity and decreased the rate of drug release [11]. Batch HG4 exhibited the highest drug release of 98.99%, likely due to its high swellability. In contrast, batch HG6 showed the lowest drug release, with only 49.57% released from the hydrogel matrix at 24 h.

To elucidate the mechanism of soframycin release, the in vitro drug release data from all batches were fitted to various kinetic models, including Zero-order, First-order, Higuchi, and Korsmeyer–Peppas. Among these, the Korsmeyer–Peppas model provided the best fit for describing the release behavior of batches HG1–HG7, as indicated by regression coefficient ($R^2$) values close to 1, reflecting a strong correlation between the experimental data and the model. The calculated release exponent ('n') values ranged from 0.59 to 0.71, suggesting that drug release from these hydrogel films followed a non-Fickian (anomalous) diffusion mechanism. This implies that the release process is governed by a combination of drug diffusion through the polymer matrix and polymer relaxation or erosion [11]. The detailed results are presented in **Table 3**.

### *3.12 Characterizations of hydrogel films*

#### *3.12.1 ATR-FTIR*

The ATR-FTIR spectra of the soframycin, CMTG, GG, HG1, unloaded HG3, and loaded HG3 hydrogel films are shown in **Figure 4A**. The ATR-FTIR spectrum of soframycin exhibited a broad absorption band at ~3250 $cm^{-1}$, which can be attributed to overlapping O–H and N–H stretching vibrations arising from multiple hydroxyl and amino groups. A characteristic peak at ~2889 $cm^{-1}$ was observed due to aliphatic C–H stretching, while a distinct band at ~1619 $cm^{-1}$ corresponded to N–H bending of primary amine groups [37]. The ATR-FTIR spectra of CMTG displayed a broad, intense absorption band at 3275 $cm^{-1}$, which indicated the –OH stretching vibrations, while the peaks at 2918 $cm^{-1}$ corresponded to the asymmetric stretching of C–H bonds. A distinct peak at 1743.39 $cm^{-1}$ indicates the presence of the ester carbonyl (C=O) group. Additionally, peaks at 1629.23 $cm^{-1}$ suggest the presence of carboxyl groups. The absorption band at approximately 1005 $cm^{-1}$ is associated with the C–O–C stretching vibration, which is characteristic of the glycosidic linkages in CMTG [12].

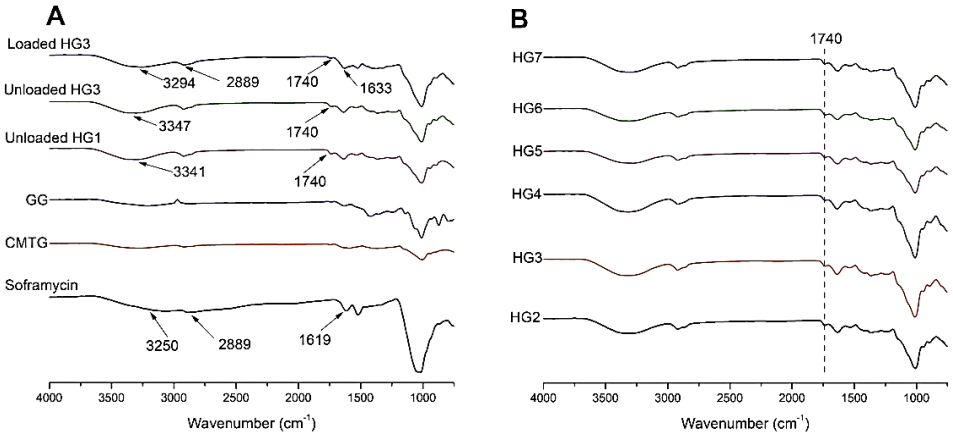


**Figure 4.** ATR-FTIR spectra of soframycin, CMTG, GG, HG1, unloaded HG3 and loaded HG3 (A) and CMTG-GG hydrogel batches HG2 to HG7 (B)

In pure GG, a broad band was observed due to the stretching vibration of -OH at 3234 $cm^{-1}$, and the peak at 2874 cm-1 corresponds to C-H stretching vibrations. The peak at 1631 $cm^{-1}$ represents the galactose and mannose ring (galactomannan sugar backbone). The peaks at 1422.31 and 1071 $cm^{-1}$ were due to the CH and O-H bending, respectively. Additional peaks at 1071.42 and 1019.84 cm-1 were assigned to C-O-C stretching and C-O stretching, respectively, owing to the pyranose ring of the galactomannan group. The peak at 872 cm-1 was attributed to C-H deformation [38, 39].

The ATR-FTIR spectra of the batch HG1 and HG3 are shown in **Figure 4A**. In batch HG1, the intensity of the -OH stretching peak increased due to enhanced hydrogen bonding. An additional peak at 1740 cm-1 was observed, which could be attributed to ester bond formation, confirming crosslinking between CMTG and CA. In batch HG3, when GG was incorporated into the CMTG hydrogel film, a more intense and broader peak was observed in the range of 3542 $cm^{-1}$ to 3049 $cm^{-1}$, which was attributed to the –OH group. The broadening of the OH band of the CMTG-GG films increased owing to intermolecular hydrogen bonding. A peak at 1740 $cm^{-1}$ was due to the stretching vibration of the ester carbonyl (C=O) group [40]. The presence of this peak confirmed the esterification reaction between CMTG and GG with citric acid [11, 38].

The ATR-FTIR spectrum of soframycin-loaded hydrogel films showed minor changes compared to pure Soframycin. The broad O–H/N–H stretching band (~3294 $cm^{-1}$) became more intense and slightly shifted, indicating hydrogen bonding between the hydroxyl and amino groups of soframycin and the hydroxyl and carboxyl groups of the hydrogel matrix. The N–H bending band (≈1619 $cm^{-1}$) was masked or shifted to 1633 $cm^{-1}$, suggesting hydrogen bonding and partial protonation/electrostatic interactions with the matrix. These spectral modifications indicate synergistic stabilization of soframycin within the CMTG–GG hydrogel through hydrogen bonding, electrostatic interactions, and network entrapment, enhancing matrix integrity and modulating drug release [37].

The ATR-FTIR spectra of batches HG2–HG7 are shown in **Figure 4B**. Considering batches HG2, HG3, and HG4, it was observed that as the GG concentration increased, the intensity of the ester carbonyl peak increased, suggesting greater GG involvement in the reaction. In the case of batch HG5-HG7, the peak of the ester carbonyl group shifted to a higher wavenumber and its intensity increased. This might be due to the increase in crosslinking density, aided by higher curing temperature, time, and CA [11]. The ATR-FTIR results were correlated with the TCC results.

### *3.12.2 Thermal analysis*

Thermogravimetric analysis was performed to analyze the thermal stability of the crosslinked hydrogel films. The TGA curves of CMTG, GG, the CMTG hydrogel film (HG1), and the CMTG-GG hydrogel film (HG3) are shown in **Figure 5**. Thermal analysis was performed over a temperature range of 30℃ to 600℃. The curves show that both CMTG and GG underwent three stages of decomposition. However, compared to CMTG, GG showed higher weight loss in the first stage of decomposition. This weight loss may be due to the dehydration of the hydroxyl (-OH) group present in the polymer. The second stage of decomposition for both polymers showed an overall similar degradation pattern, with a major weight loss. This occurs because, after the water molecules are removed, the polymer's main structure begins to break down at a certain temperature. This leads to the breakdown of the polymer backbone and significant weight loss [11].

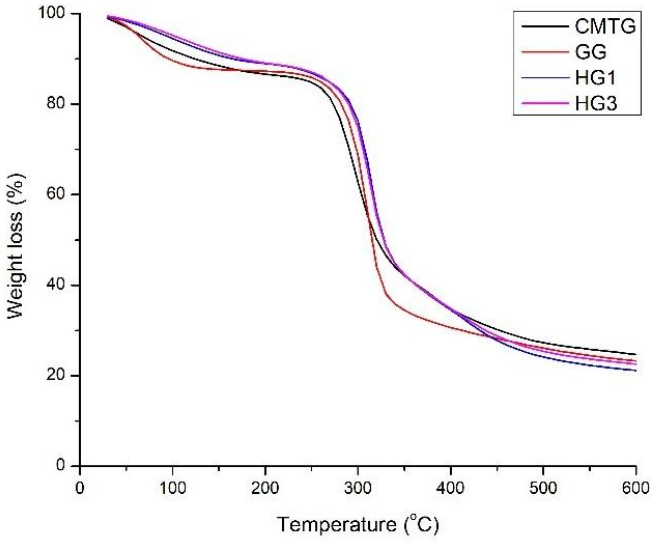


**Figure 5.** TGA thermograms of CMTG, GG, HG1, and HG3

At the end of the second stage, a sharp weight loss was observed in the GG group. The third stage of degradation was slow, but weight loss continued. The overall results indicated that the thermal stability of CMTG was higher than that of GG, which may be due to the chemical modification of CMTG, providing better thermal stability [12].

The TGA curves of the CMTG hydrogel film (HG1) and CMTG-GG hydrogel film (HG3) showed slight weight loss of up to 10-15 % at 280℃, which might be due to the loss of moisture from the hydrogel films. No significant difference was observed between batches in the first stage. The second stage of decomposition started at 280℃ and ended at 400℃. This region represents the thermal degradation of the polymer chain backbone of CMTG and GG. The TGA curves of HG1 and HG3 show that incorporating GG into the CMTG hydrogel film enhances the thermal stability of the films. Batch HG3 showed higher thermal stability than HG1. This may be because an increase in the concentration of GG leads to greater participation in the crosslinking reaction, providing more thermal stability to hydrogel films [36, 41, 42].

## 4. Conclusıon

In the present study, we successfully developed soframycin-loaded CMTG-GG hydrogel films via solution casting. The effects of varying ratios of CMTG and GG polymers, CA concentrations, curing temperature, and curing time on various properties, including hydrogel film swelling, were evaluated. Incorporating GG into CMTG improved the total carboxyl content (TCC), hydrophilicity, swelling, drug loading, and release. The findings revealed that increasing curing temperature, time, and CA concentration decreased swelling, loading, and release. The optimized batch (HG3) showed the highest swelling and drug loading. The crosslinked films exhibited low protein adsorption (<0.5 mg/cm$^2$), good biocompatibility, and effective microbial barrier properties. ATR-FTIR confirmed ester crosslinking, and TGA results indicated the thermal stability. The crosslinked hydrogel films made from CMTG-GG exhibited higher swelling than the CMTG-PVA hydrogel films. The results indicate that combining GG with CMTG increases the swelling capacity of the hydrogel films. The soframycin-loaded CMTG-GG hydrogel film demonstrated good drug release behavior, making it a promising candidate for drug delivery. Further *in vivo* studies can help confirm whether the soframycin-loaded CMTG-GG hydrogel films are safe and effective for biomedical applications.

## Acknowledgements

The authors are thankful to Adv. Vaibhav (Dada) Patil, President of the Loknete Hon. Hanmantrao Patil Charitable Trust, Vita, for providing the necessary facilities to carry out this research. Shivaji University, Kolhapur; Krishna Vishwa Vidyapeeth, Karad; and Sadguru Gadage Maharaj College, Karad are acknowledged for their assistance with analytical work.

## Conflict of interest

The authors declare that they have no competing interests.

## Data availability

The data supporting the findings of this study will be made available by the corresponding author upon reasonable request.

## Authors Contributions

V.S.G: Project planning, Investigation, Data curation, Review, and editing
K.K.M: Project administration, Investigation, Conceptualization, Review, and editing
V.D.H: Methodology, Resources, Formal analysis, Data curation, Software.
A.U.S.: Methodology, Investigation, Visualisation, Writing original draft.
O.S.V: Methodology, Investigation, Visualisation, Writing original draft.
R.J.D: Visualization, Supervision, Statistics, Review and editing.

## Authors Orcid numbers:

Vishwajeet Sampatrao Ghorpade: 0000-0002-7324-3666
Kailas Krishnat Mali: 0000-0002-1789-3592
Vijay Daulatrao Havaldar: 0009-0006-7092-5609
Afroj Usman Shikalkar: 0009-0009-2488-3753
Om Santosh Varude: 0009-0006-7704-5903
Remeth Jacky Dias: 0000-0002-8234-9630

## Funding

The authors acknowledge that no funding was received to support this study.

## Using artificial intelligence chatbots

Artificial intelligence chatbots were used only for language editing and improvement of grammar during manuscript preparation. The authors take full responsibility for the content of the article.

## References

1. Almoshari YH. Novel Hydrogels for Topical Applications: An Updated Comprehensive Review Based on Source. Gels (2022) 8(3):1–24.
2. Raina N, Pahwa R, Bhattacharya J, Paul AK, Nissapatorn V, Pereira MDL, et al. Drug Delivery Strategies and Biomedical Significance of Hydrogels: Translational Considerations. Pharmaceutics (2022)14(3):1–31.
3. Narayanaswamy R, Torchilin VP. Hydrogels and their applications in targeted drug delivery. Molecules (2019) 24(3):1–18.
4. Maleki B, Ghamari Kargar P, Sedigh Ashrafi S, Ghani M. Perspective Chapter: Introduction to Hydrogels - Definition, Classifications, Applications and Methods of Preparation. In: Ionic Liquids - Recent Advances. IntechOpen (2024) p. 1–27.
5. Salunkhe NH, Mali KK, Sidwadkar PH, Pareek KM, Aundhakar AS. Synthesis and characterization of citric acid crosslinked garden cress seeds mucilage hydrogel for controlled drug release. J Drug Deliv Sci Technol (2025) 112:107270.
6. Umar M, Khan A, Azhar M, Faizal M, Abdullah B, Al-arjan WS, et al. Hydrogels : Classifications , fundamental properties , applications , and scopes in recent advances in tissue engineering and regenerative medicine – A comprehensive review. Arab J Chem (2024)17(10):105968.
7. Nimbekar TP, Bhange PG, Wanjari BE, Mehere AP. Formulation and evaluation of some framycetin sulphate ointment. Int J Pharma Bio Sci (2012) 3(2):327–32.
8. Stidolph NE, Alston JM. The use of soframycin (framycitin sulphate) for intestinal sterilization. Gut (1960)1(4):323–5.
9. Mali NV, Bansode DA. Stability indicating thin-layer chromatographic determination of framycetin sulphate as bulk drug: Application to forced degradation study. Int J PharmTech Res (2016) 9(9):189–99.
10. Clarot I, Regazzeti A, Auzeil N, Laadani F, Citton M, Netter P, et al. Analysis of neomycin sulfate and framycetin sulfate by high-performance liquid chromatography using evaporative light scattering detection. J Chromatogr (2005) 1087(1–2):236–44.
11. Mali KK, Ghorpade VS, Dias RJ, Dhawale SC. Synthesis and characterization of citric acid crosslinked carboxymethyl tamarind gum-polyvinyl alcohol hydrogel films. Int J Biol Macromol (2023) 236:123969.
12. Mali KK, Dhawale SC, Dias RJ. Synthesis and characterization of hydrogel films of carboxymethyl tamarind gum using citric acid. Int J Biol Macromol (2017) 105:463–70.
13. Mali KK, Dhawale SC, Dias RJ, Havaldar VD, Kavitake PR. Interpenetrating networks of carboxymethyl tamarind gum and chitosan for sustained delivery of aceclofenac. Marmara Pharm J (2017) 21(4):771–82.
14. Dehghani Soltani M, Meftahizadeh H, Barani M, Rahdar A, Hosseinikhah SM, Hatami M, et al. Guar (Cyamopsis tetragonoloba L.) plant gum: From biological applications to advanced nanomedicine. Int J Biol Macromol (2021) 193:1972–85.
15. Morais MAP, Silva M, Barros M, Halley P, Almeida Y, Vinhas G. Impact of citric acid on guar gum carboxymethylcellulose crosslinked blend films. J Appl Polym Sci (2024) 141(44):1–14.
16. Khushbu, Warkar SG. Potential applications and various aspects of polyfunctional macromolecule- carboxymethyl tamarind kernel gum. Eur Polym J (2020) 140:110042.
17. Rani I, Warkar SG, Kumar A. Synthesis and characterization of novel carboxymethyl tamarind kernel gum - Poly (vinyl alcohol)/guar gum-based hydrogel film loaded with ciprofloxacin for biomedical applications. Int J Biol Macromol (2024) 282:136766.
18. Mali KK, Dhawale SC, Dias RJ, Ghorpade VS. Delivery of drugs using tamarind gum and modified tamarind gum: A review. Bull Fac Pharmacy, Cairo Univ (2019) 57(1):1–24.
19. Shaw GS, Biswal D, Anupriya B, Banerjee I, Pramanik K, Anis A, et al. Preparation, Characterization and Assessment of the Novel Gelatin-Tamarind Gum / Carboxymethyl Tamarind Gum Based Phase-Separated Films for Skin Tissue Engineering Applications. Polym Plast Technol Eng (2017) 56(2):141-152.
20. Li K, Zhu J, Guan G, Wu H. Preparation of chitosan-sodium alginate films through layer-by-layer assembly and ferulic acid crosslinking: Film properties, characterization, and formation mechanism. Int J Biol Macromol (2019)122:485–92.

21. Mali KK, Dhawale SC, Dias RJ, Dhane NS, Ghorpade VS. Citric Acid Crosslinked Carboxymethyl Cellulose-based Composite Hydrogel Films for Drug Delivery. Indian J Pharm Sci (2018) 80(4):657–67.
22. Ramachandra H, Kumari L, Maiti S, Sakure K, Nakhate KT, Tiwari V, et al. A review on challenges and issues with carboxymethylation of natural gums : The widely used excipients for conventional and novel dosage forms. Int J Biol Macromol (2022) 209:2197–212.
23. Bhubhanil S, Talodthaisong C, Khongkow M, Namdee K, Wongchitrat P, Yingmema W, et al. Enhanced wound healing properties of guar gum/curcumin-stabilized silver nanoparticle hydrogels. Sci Rep (2021) 11(1):21836.
24. Keshawy M, Kamal RS, Abdelhamid AE, Labena A, Amin A, Hasan AM, et al. Novel green sustainable hydrogel composites based on guar gum and algal species for wastewater remediation. Int J Environ Sci Technol (2025) 22(10):8895–918.
25. Tripathi J, Ambolikar R, Gupta S, Jain D, Bahadur J, Variyar PS. Methylation of guar gum for improving mechanical and barrier properties of biodegradable packaging films. Sci Rep (2019) 9(1):14505.
26. Abdel-raouf ME. Current Research in Biopolymers Guar Gum Based Hydrogels for Sustained Water Release Applications in Agriculture , a Review. Curr Res Biopolym (2019) 2(01):1–15.
27. Ghauri ZH, Islam A, Qadir MA, Gull N, Haider B, Khan RU, et al. Development and evaluation of pH-sensitive biodegradable ternary blended hydrogel films (chitosan/guar gum/PVP) for drug delivery application. Sci Rep (2021) 11(1):21255.
28. Bernal-Chávez SA, Alcalá-Alcalá S, Almarhoon ZM, Turgumbayeva A, Gürer ES, De Los Dolores Campos-Echeverria M, et al. Novel ultra-stretchable and self-healing crosslinked poly (ethylene oxide)-cationic guar gum hydrogel. J Biol Eng (2023) 17(1):64.
29. Bandyopadhyay S, Saha N, Brodnjak UV, Sáha P. Bacterial cellulose and guar gum based modified PVP-CMC hydrogel films: Characterized for packaging fresh berries. Food Packag Shelf Life (2019) 22:100402.
30. Ghorpade VS, Mali KK, Dias RJ, Dhawale SC, Digole RR, Gandhi JM, et al. Citric acid crosslinked hydroxyethyl tamarind gum-based hydrogel films: A promising biomaterial for drug delivery. Int J Biol Macromol (2024) 282(P4):137127.
31. Mastiholimath VS, Valerie CTW, Mannur VS, Dandagi PM, Gadad AP, Khanal P. Formulation and evaluation of solid lipid nanoparticle containing silver sulfadiazine for second and third degree burn wounds and its suitable analytical method development and validation. Indian J Pharm Educ Res (2020) 54(1):31–45.
32. Zarbab A, Sajjad A, Rasul A, Jabeen F, Javaid Iqbal M. Synthesis and characterization of Guar gum based biopolymeric hydrogels as carrier materials for controlled delivery of methotrexate to treat colon cancer. Saudi J Biol Sci (2023) 30(8):1–11.
33. Mohammad Mahdi Dadfar S, Kavoosi G, Mohammad Ali Dadfar S. Investigation of mechanical properties, antibacterial features, and water vapor permeability of polyvinyl alcohol thin films reinforced by glutaraldehyde and multiwalled carbon nanotube. Polym Compos (2014) 35(9):1736–43.
34. Li X, Wu W, Wang J, Duan Y. The swelling behavior and network parameters of guar gum / poly (acrylic acid) semi-interpenetrating polymer network hydrogels. Carbohydr Polym (2006) 66:473–9.
35. Das A, Wadhwa S, Srivastava AK. Crosslinked Guar Gum Hydrogel Discs for Colon-Specific Delivery of Ibuprofen : Formulation and In Vitro Evaluation. Drug Deliv (2006) 13:139–42.
36. Daud H, Ghani A, Iqbal DN, Ahmad N, Nazir S, Muhammad MJ, et al. Preparation and characterization of guar gum based biopolymeric hydrogels for controlled release of antihypertensive drug. Arab J Chem (2021)14(5):103111.
37. Wu Z, Yaqoob I, Afzal M, Iqbal FM, Hassan W, Chen X. Evaluation and characterization of framycetin sulphate loaded hydrogel dressing for enhanced wound healing. PLoS One (2025) 20(4):e0317273.
38. Kumar A, De A, Mozumdar S. Synthesis of acrylate guar-gum for delivery of bio-active molecules Synthesis of acrylate guar-gum for delivery of bio-active molecules. Bull Mater Sci (2015) 28(4):1025–32.
39. Elsaeed SM, Zaki EG, Omar WAE, Soliman AA, Attia AM. Guar Gum-Based Hydrogels as Potent Green Polymers for Enhanced Oil Recovery in High-Salinity Reservoirs. ACS omega (2021) 6:23421–31.
40. Banegas RS, Zornio CF, De Borges AMG, Porto LC, Soldi V. Preparation, characterization and properties of films obtained from crosslinked guar gum. Polimeros (2013) 23(2):182–8.
41. Mohammadi H, Alihosseini F, Hosseini SA. Improving physical and biological properties of nylon monofilament as suture by Chitosan/Hyaluronic acid. Int J Biol Macromol (2020) 164:3394–402.
42. Chen JC, Tseng WY, Tseng IH, Tsai MH. High Transparency and Thermal Stability of Alicyclic Polyimide with Crosslinking Structure by Triallylamine. Adv Mater Res (2011) 287–290:1388–96.